
Article:
Kadochnikova, A. orcid.org/0000-0002-5416-7848 and Kadirkamanathan, V. orcid.org/0000-0002-4243-2501 (2023) Estimation of potential field environments from heterogeneous behaviour of sensing agents. IET Signal Processing, 17 (1). e12181. ISSN 1751-9675

https://doi.org/10.1049/sil2.12181

Received: 6 January 2022 | Revised: 12 November 2022 | Accepted: 29 November 2022

DOI: 10.1049/sil2.12181

IET Signal Processing

The Institution of Engineering and Technology WILEY

ORIGINAL RESEARCH

Estimation of potential field environments from heterogeneous behaviour of sensing agents

Anastasia Kadochnikova | **Visakan Kadirkamanathan**

Department of Automatic Control and Systems Engineering, University of Sheffield, Sheffield, UK

Correspondence

Visakan Kadirkamanathan, Department of Automatic Control and Systems Engineering, University of Sheffield, Sheffield S1 3JD, UK.
Email: visakan@sheffield.ac.uk

Present address

Anastasia Kadochnikova, School of Biosciences, University of Nottingham, Sutton Bonington, Loughborough LE12 5RD, UK

Funding information

Full Departmental Scholarship of ACSE Department, University of Sheffield

Abstract

This paper proposes a novel modelling framework for estimating the global potential field from trajectories of multiple sensing agents whose perception of the unknown field is subject to abrupt changes. We derive a parametrised formulation of the estimation problem by combining the jump Markov non-linear system (JMNLS) model of agent dynamics with a basis function decomposition of the environmental field. An approximate expectation-maximisation algorithm is employed for joint estimation of the global field and of the agent behavioural modes from observed agent trajectories. To avoid prohibitive computational costs associated with the state estimation of JMNLS, we utilise two approximation steps. First, an interacting multiple model smoother is used to account for the hybrid structure that emerges in this problem. Second, we propose two approaches to approximating the non-linear sufficient statistics during the expectation step. This results in the maximization step being exact. The performance of the developed framework is tested on simulation examples and demonstrated on an application study in which the observed movement patterns of immune cells are utilised in quantifying the underlying chemical concentration field that governs their migration. The results showcase that the proposed framework can be readily applied to problems where agents assume several behavioural modes.

KEYWORDS

hidden Markov models, maximum likelihood estimation, nonlinear dynamical systems, parameter estimation, state estimation

1 | INTRODUCTION

The phenomena in which the physical environment influences the movement of sensing agents are encountered in a multitude of applications ranging from environmental engineering to cell biology. Arrays of moving sensors used for source localisation in spillages and environmental surveys correct their trajectories based on point-wise measurements of local concentrations [1, 2]. In particle physics, trajectories of Brownian particles drift in response to unobserved microscopic force fields [3]. In biological applications, cell migration is driven by attractive or repelling chemical concentrations [4, 5]. The common assumption in modelling these phenomena is that the environment is acting on sensing agents as a potential field, forcing a sensor to align with the direction of the steepest gradient. The potential field paradigm has long been used in robot path planning [6] and other applications where a single moving object is moving in response to its surroundings [7, 8]. The emergent challenge of using potential fields to model physical phenomena is that the acting environment cannot be observed directly and is sensed only locally by individual agents. However, with the large number of agents sensing to the same potential field, it is possible to infer its underlying gradient from the general trends in the direction of sensor motion. This paper addresses the problem of estimating the hidden global potential field from the trajectories of multiple sensing agents.

Reconstructing the global potential field from the localised trajectories is an infinite-dimensional estimation problem that

is further complicated by the lack of knowledge about the functional form that best represents the field. Existing solutions range from approximating the gradient locally [1] to fitting *a priory* chosen functions to the data [9], to considering a partial differential equation that governs the field and estimating its parameters [10]. Models of the environmental field without prior assumptions about its functional form rely on basis function decomposition, which yields a linear-in-parameters representation [4, 11, 12]. In Refs. [4, 11], frequentist approaches are adopted to estimate scaling coefficients of the basis function grid that approximates the concentration of a signalling substrate. Authors of Ref. [12] propose a hierarchical Bayesian framework for field inference that performs the order reduction of the basis function grid and parameter estimation simultaneously. All of the existing solutions rely on the assumption that the behaviour of moving agents is homogeneous and they respond to the environment at all times. However, in most real-life applications, the perception of the environment by an agent is prone to abrupt changes that can be caused, amongst other reasons, by component failures, sensing faults [13], or physiological limitations of an agent [14, 15]. The present paper summarises the first attempt to extend the environmental inference to the cases of heterogeneous sensing behaviour of mobile agents.

We consider a novel class of problems that accounts for the fact that environmental sensing by a single agent is an intermittent process: not only the environment is unobserved but it is unknown whether an individual agent at a given time is interacting with it. Our principal contribution is a rigorous estimation framework that scales to a large number of agents and their possible behaviors. The problem of agent localization is not considered here, nor is the agent-to-agent interaction. It is assumed that the agents do not have control of their own behavior and cannot exchange information about the underlying environment with each other.

We approach this problem by formulating a hybrid model of the single agent motion. The abrupt changes in agent's perception of the environment are modelled by a Markov chain that evolves according to the unknown transition probability matrix. The state of this Markov chain correspond to behavioural modes, each described by a generic non-linear state-space model (SSM) [16]. The influence of the environment is modelled by the input signal of the SSM. The environmental sensing mechanism within an individual agent is not considered here—we treat agent movement as the direct response to the sensed gradient. This way, the only strict assumption we impose on the dynamical model is that it is linear with respect to the input signal. Limited knowledge about the agent's behaviour is reflected by the partially hidden state and the unobserved sequence of the governing Markov chain. The resultant model is the input-affine jump Markov non-linear system (JMNLS) that remains linear with respect to the unknown parameters of the environment model. The joint problem of state parameter estimation of JMNLS can be decoupled and solved within the maximum likelihood (ML) setting via the offline expectation-maximisation (EM) algorithm [17–20], leading to a closed-form expression for field parameter estimates in terms of several sufficient statistics which are non-linear with respect to. agent states. These expressions will hold for a broad class of dynamical systems meaning that our framework can be readily used in a range of applications.

The main challenge of implementing the framework is associated with computing the expectations for sufficient statistics, because evaluation of smoothing probability density functions (*pdf*s) of hidden data requires storing exhaustive mode histories, incurring exponential computational costs [21]. Multiple methods of feasible jump Markov system (JMS) estimation have been proposed, mostly in application to jump Markov linear systems. They can be divided into two broad categories: the multiple model (MM) methods [22] and particle-based methods [23]. The MM approaches run banks of mode-associated filters in parallel and approximate mode histories by a single Gaussian at the end of every recursion [24]. The most popular approach is the interacting multiple model (IMM) filtering [25, 26]. Particle-based algorithms rely on sampling from complex state *pdf*s using sequential Monte Carlo (SMC) methods [23, 27, 28]. An alternative solution that does not quite fall into either of the categories is proposed in Ref. [29] in the form of iterating optimal estimators for the continuous and discrete states.

Only a limited number of works deal directly with JMNLS. Several extensions of the IMM framework to non-linear cases have been proposed, employing banks of extended [30], unscented [31], and cubature [32] filters. In Ref. [33], a Rao–Blackwellised particle filter (RBPF) is presented that marginalizes over modes and uses classical SMC for the states, leading to particle depletion around mode changes. Authors of Ref. [34] avoid particle degeneracy by employing IMM-type particle filter. The IMM smoothing strategies for JMNLS require an additional approximation of the joint pdf for state and mode in backward time. Existing solutions rely on two-filter approach to compute mode-interacting likelihoods [35, 36], or on backward kernel approximation under small noise assumption [37, 38]. An improved method based on the closed-form backward recursion of the joint state-mode posterior has been proposed during the preparation of this manuscript in Ref. [39].

To our best knowledge, the only particle forward-backward estimator of JMNLS in the parameter estimation context has been proposed as part of the online EM procedure in Ref. [40]. The method combines RBPF with conditional Hidden Markov model filters in forward recursion to avoid particle degeneracy around mode changes. At backward recursion, the authors compare a path-based particle smoother that 'prunes' unlikely modes [41] and computationally expensive forward particle smoother. The uthors state that the use of path-based smoother leads to particle degeneracy, but explain that its effect is not as severe in the context of the online EM algorithm. For offline problems, this is detrimental because the state estimator stops detecting agent mode switches as particles deplete and estimation errors accumulate, with agents becoming 'stuck' in an insensitive mode. On the other hand, forward smoothing does not scale well to large number of agents as its complexity quadruples with the growing numbers

of particles. To ensure scalability of the filed inference framework to a large set of sensing agents, we employ IMM-type smoothing to avoid particle degeneracy altogether. Gaussian approximations of posterior *pdf*s produced by the IMM smoother are used to compute the non-linear sufficient statistics either numerically using direct importance sampling from these *pdf*s or analytically by exploiting the adopted model parametrisation and mean-field (MF) approach.

The remainder of this paper is structured as follows. Section 2 introduces a hybrid model of individual agent dynamics that incorporates the influence of the environment. The problem of estimating the environment from multiple agent trajectories is then formulated in the ML setting. Section 3 details the estimation procedure and discusses adopted approximations. The estimation performance is demonstrated on a simulated data in Section 4. Section 5 demonstrates how the proposed modelling framework can be applied to the experimental data collected from observing immune cell migration in the inflammation process. Conclusions are drawn in Section 6.

2 | MODEL OF AGENT-ENVIRONMENT INTERACTION

2.1 | Agent dynamics

Let $\mathbb{M} = \{1, \dots, \mathrm{N}\}$ be the countable finite set corresponding to possible behavioral modes that can be assumed by an individual sensing agent. In the collection of K agents, the discrete time dynamics and observation process of the kth agent are described by an input affine hybrid system.

$$\boldsymbol{r}^{\mathrm{k}}_{\mathrm{t}+1} \sim \Phi\left(\boldsymbol{r}^{\mathrm{k}}_{\mathrm{t}+1} \mid \boldsymbol{r}^{\mathrm{k}}_{\mathrm{t}}\right) \tag{1a}$$

$$\boldsymbol{x}^{\mathrm{k}}_{\mathrm{t}+1} = f_{(\boldsymbol{r}^{\mathrm{k}}_{\mathrm{t}})}\left(\boldsymbol{x}^{\mathrm{k}}_{\mathrm{t}}\right) + g_{(\boldsymbol{r}^{\mathrm{k}}_{\mathrm{t}})}\left(\boldsymbol{x}^{\mathrm{k}}_{\mathrm{t}}\right)\boldsymbol{u}^{\mathrm{k}}_{\mathrm{t}} + \mathbf{G}_{(\boldsymbol{r}^{\mathrm{k}}_{\mathrm{t}})}\boldsymbol{w}^{\mathrm{k}}_{\mathrm{t}} \tag{1b}$$

$$\boldsymbol{y}^{\mathrm{k}}_{\mathrm{t}} = h_{(\boldsymbol{r}^{\mathrm{k}}_{\mathrm{t}})}\left(\boldsymbol{x}^{\mathrm{k}}_{\mathrm{t}}\right) + \boldsymbol{v}^{\mathrm{k}}_{\mathrm{t}}, \tag{1c}$$

where $\boldsymbol{r}^{\mathrm{k}}_{\mathrm{t}} \in \mathbb{M}$ is the modular state or mode that changes according to some kernel Φ and where $\boldsymbol{x}^{\mathrm{k}}_{\mathrm{t}+1} \in \mathbb{R}^{2d}$ is the continuous-valued state vector that consists of the spatial position and velocity projections on d axes

$$\boldsymbol{x}^{\mathrm{k}}_{\mathrm{t}+1} = \left[s^{\mathrm{k}}_{\mathrm{t},1}, \dots, s^{\mathrm{k}}_{\mathrm{t},d}, v^{\mathrm{k}}_{\mathrm{t},1}, \dots, v^{\mathrm{k}}_{\mathrm{t},d}\right]^{\top},$$

where $(\cdot)^{\top}$ denotes the transpose operator. Both states and modes are latent and are observed indirectly through the measured agent position $\boldsymbol{y}^{\mathrm{k}}_{\mathrm{t}} \in \mathbb{R}^{d}$. Further in Equation (1), $\mathbf{G}_{(\boldsymbol{r}^{\mathrm{k}}_{\mathrm{t}})}$ is the noise input gain, $\boldsymbol{w}^{\mathrm{k}}_{\mathrm{t}} \sim \mathcal{N}\left(0, \mathbf{Q}_{(\boldsymbol{r}^{\mathrm{k}}_{\mathrm{t}})}\right)$, $\mathbf{Q}_{(\boldsymbol{r}^{\mathrm{k}}_{\mathrm{t}})} \in \mathbb{R}^{2d\times 2d}$ and $\boldsymbol{v}^{\mathrm{k}}_{\mathrm{t}+1} \sim \mathcal{N}(0, \mathbf{R})$, $\mathbf{R} \in \mathbb{R}^{d\times d}$ are mutually independent Gaussian noises, and the input vector $\boldsymbol{u}^{\mathrm{k}}_{\mathrm{t}}$ reflects the influence of the hidden global environment $\mathcal{U}$.

In JMSs, switching between modes is governed by a homogeneous ergodic Markov chain with initial probabilities $\Pi = \left\{\boldsymbol{\pi}_{\mathrm{j}} \geq 0\right\}_{\mathrm{j}=1}^{\mathrm{N}}$ and with the transition probability matrix $\Phi = \left\{\boldsymbol{\phi}_{\mathrm{ji}} \geq 0\right\}_{\mathrm{i,j}=1}^{\mathrm{N}}$ elements of which are defined as follows:

$$\boldsymbol{\phi}_{\mathrm{ji}} \triangleq \mathrm{P}\left(\boldsymbol{r}^{\mathrm{k}}_{\mathrm{t}+1} = \mathrm{i} \mid \boldsymbol{r}^{\mathrm{k}}_{\mathrm{t}} = \mathrm{j}\right),$$

where $\mathrm{j}, \mathrm{i} \in \mathbb{M}$. Since the mode sequence is unobserved, matrix Φ cannot be evaluated directly and is assumed to be unknown.

Additional properties of the model Equation (1) are defined by the following assumptions.

Assumption 1 *The mode transition process is right-continuous,* that is, *the effect of mode* $\boldsymbol{r}^{\mathrm{k}}_{\mathrm{t}}$ *starts at* t^{+}.

Assumption 2 *The initial state of the* kth *object* $\boldsymbol{x}^{\mathrm{k}}_{0} \sim \mathcal{N}\left(\widehat{\boldsymbol{x}}^{\mathrm{k}}_{0}, \mathbf{P}^{\mathrm{k}}_{0}\right)$ *is independent from* $\boldsymbol{w}^{\mathrm{k}}_{\mathrm{t}+1}$ *and* $\boldsymbol{v}^{\mathrm{k}}_{\mathrm{t}+1}$ $\forall$ t.

Assumption 3 *Parameters of the candidate SSMs*

$$f_{(\mathrm{j})}(\cdot), g_{(\mathrm{j})}(\cdot), \mathbf{G}_{(\mathrm{j})}, h_{(\mathrm{j})}(\cdot), \quad \forall \mathrm{j} \in \mathbb{M} \tag{2}$$

and the initial state and mode of each agent $\left(\boldsymbol{r}^{\mathrm{k}}_{0}, \boldsymbol{x}^{\mathrm{k}}_{0}\right)$, $\mathrm{k} = 1, \dots, \mathrm{K}$ *are known.*

Assumption 4 *The process of observing agent positions is mode-independent.*

$$h_{(\mathrm{j})}(\cdot) = h(\cdot) \quad \forall \mathrm{j} \in \mathbb{M}$$

Note that Assumptions 1–2 are standard for JMS and 3–4 are non-strict. The relaxation for Assumption 3 is discussed further in Remark 1. Assumption 4 is reasonable for a wide class of applications because agent positions are often observed externally (GPS for sensors and robots and video-microscopy for cells), thus the changes in the agent's behavior do not affect the measurement process.

Remark 1 *The unknown vector* Θ *is not limited to the parameters considered in this study and may be extended to include initial conditions, parameters of the noise distributions* $\left(\mathbf{R}, \mathbf{Q}_{(\mathrm{j})}, \mathrm{j} \in \mathbb{M}\right)$, *or dynamical models* $\left(f_{(\mathrm{j})}(\cdot), g_{(\mathrm{j})}(\cdot), h_{(\mathrm{j})}(\cdot), \mathrm{j} \in \mathbb{M}\right)$ *thus relaxing* 3. *The estimation of the former is straightforward and of the latter is case-specific. Under Gaussian assumptions, the maximum likelihood estimates (MLEs) of the noise distribution parameters can be obtained in closed form by extending the M-step with a series of conditional optimization problems. This modification results in the familiar Expectation-Conditional Maximization (ECM) scheme* [42].

The causal relationships between states, modes, and observations for an individual agent under the adopted assumptions are illustrated in Figure 1. For each agent the continuous state sequence is denoted by $\mathbf{x}^{\mathrm{k}} \triangleq \left\{\boldsymbol{x}^{\mathrm{k}}_{\mathrm{t}}\right\}_{\mathrm{t}=1}^{\mathrm{T^k}}$ and the mode

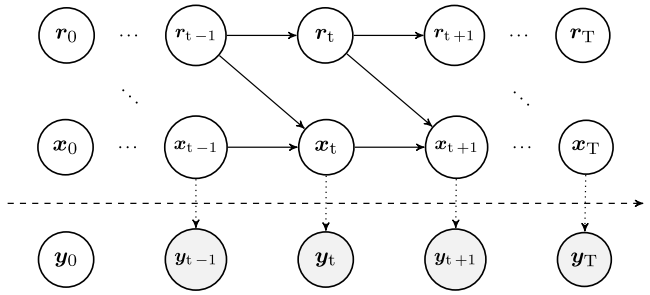

FIGURE 1 Directed acyclic graph of the considered jump Markov system. The observation $\boldsymbol{y}_t$ depends only on the state $\boldsymbol{x}_t$, while the state update is conditioned by the previous mode $\boldsymbol{r}_{t-1}$ and the previous state $\boldsymbol{x}_{t-1}$.

sequence is $\mathbf{r}^k \triangleq \{\boldsymbol{r}_t^k\}_{t=1}^{T^k}$, where T^k is the length of the observation period for the kth agent. The hidden data set comprises the collections of state and mode sequences over K agents $\mathcal{X} = \{\mathbf{x}^k\}_{k=1}^K, \mathcal{R} = \{\mathbf{r}^k\}_{k=1}^K$.

2.2 | Environment parametrization

The input vector in Equation (1b) represents the influence of the global environment acting as a potential field

$$\boldsymbol{u}_t^k = \nabla \mathcal{U}\left(s_{t,1}^k, \ldots, s_{t,d}^k\right), \tag{3}$$

where $s_{t,1}^k, \ldots, s_{t,d}^k$ is the spatial position of kth agent at time instance t. Since the problem of environment estimation often occurs in applications with slowly diffusing chemical or physical fields, it is reasonable to assume the following:

Assumption 5 *The hidden environment $\mathcal{U}$ is a smooth time-invariant function of coordinates $(s_1, \ldots, s_d)$.*

Assumption 5 is commonly adopted in estimation frameworks where the environment is invariant [7] or agents move with rates that are much larger than the diffusion rate of the field [4, 11, 12], unless the field is explicitly modeled by the partial differential equation, such as [10]. Another common assumption when it comes to networks of sensors, particles, or cells is that their tracking is preformed independently from their interaction with the environment:

Assumption 6 *Sufficient tracking data $\mathcal{Y} = \{\mathbf{y}^k\}_{k=1}^K$ is collected prior to the inference.*

Estimating $\mathcal{U}$ directly poses an infinite-dimensional problem. A natural way to make this problem tractable is to represent the smooth function $\mathcal{U}$ by a linear combination of M isotropic differentiable basis functions via the following decomposition

$$\mathcal{U}(s_{t,1}, \ldots, s_{t,d}) = \mathcal{U}_0 + \sum_{m=1}^{M} \beta_m(s_{t,1}, \ldots, s_{t,d})\theta_m, \tag{4}$$

where β_m denotes a multivariate basis function defined in d dimensions and θ_m is the corresponding scaling coefficient that determines the magnitude of the function and where $\mathcal{U}_0$ is an additive constant.

Remark 2 *The unknown potential field is only identifiable up to an additive constant $\mathcal{U}_0$ since it is not the magnitude of the field that drives agent movement but its gradient.*

With the choice of Equation (4), Equation (3) becomes

$$\boldsymbol{u}_t^k = \nabla\varphi(\boldsymbol{x}_t^k)\boldsymbol{\theta}, \tag{5}$$

where the term $\nabla\varphi(\boldsymbol{x}_{t+1}^k)$ denotes the gradient of superposition of basis functions at the current agent location

$$\nabla\varphi(\boldsymbol{x}_t^k) = \begin{bmatrix} \dfrac{\partial\beta_m(s_{t,1}, \ldots, s_{t,d})}{\partial s_{t,d}} \\ \cdots \\ \dfrac{\partial\beta_m(s_{t,1}, \ldots, s_{t,d})}{\partial s_{t,d}} \end{bmatrix}_{m=1}^{M}, \tag{6}$$

and where $\boldsymbol{\theta}$ contains corresponding scaling coefficients

$$\boldsymbol{\theta} = [\theta_1, \ldots, \theta_m, \ldots, \theta_M]^\top,$$

thus the inference of the unknown global field becomes the problem of estimating $\boldsymbol{\theta}$. By denoting $\widetilde{g}_{(\boldsymbol{r}_t^k)} \triangleq g_{(\boldsymbol{r}_t^k)}(\boldsymbol{x}_t^k)\nabla\varphi(\boldsymbol{x}_t^k)$, we can rewrite the model of agent dynamics Equation (1b) explicitly as a linear function of the unknown field parameters

$$\boldsymbol{x}_{t+1}^k = f_{(\boldsymbol{r}_t^k)}(\boldsymbol{x}_t^k) + \widetilde{g}_{(\boldsymbol{r}_t^k)}(\boldsymbol{x}_t^k)\boldsymbol{\theta} + \mathbf{G}_{(\boldsymbol{r}_t^k)}\boldsymbol{w}_t^k, \tag{7}$$

which will allow us to the obtain a closed form expression of the environment model parameters in further subsections.

3 | ESTIMATION FRAMEWORK

3.1 | Expectation-maximisation algorithm

The task of hidden environment estimation associated with the presented model can be formalised as two coupled estimation problems: (i) estimate the latent variables $\{\mathcal{X}, \mathcal{R}\}$ given the tracking data $\mathcal{Y}$; (ii) estimate the unknown parameter set $\Theta = \{\Phi, \boldsymbol{\theta}\}$ given the tracking data $\mathcal{Y}$.

In the context of the EM estimation for the model described above, there exists a complete data set $\mathcal{Z} = \{\mathcal{R}, \mathcal{X}, \mathcal{Y}\}$. Then MLEs of the unknown parameters can be obtained recursively by maximising the log-likelihood function of $\mathcal{Z}$:

$$\mathcal{L}(\Theta) = \log p(\mathcal{Z} \mid \Theta), \tag{8}$$

which is usually lower bounded by its conditional expectation

$$\mathcal{Q}\left(\Theta, \widehat{\Theta}^{l-1}\right) = \mathbb{E}_{\mathcal{R},\mathcal{X}}\left[\mathcal{L}(\Theta) \mid \mathcal{Y}, \widehat{\Theta}^{l-1}\right], \tag{9}$$

where $\mathbb{E}[\cdot]$ denotes the expected value of the function and where $\widehat{\Theta}^{l-1}$ is the MLE of unknown parameters obtained at the previous iteration of the EM algorithm. The subscript $\mathcal{R}, \mathcal{X}$ in the expectation indicates that it is taken over the joint hidden data *pdf* which we denote it as follows:

$$\boldsymbol{q}(\mathcal{R}, \mathcal{X}) \triangleq p\left(\mathcal{R}, \mathcal{X} \mid \mathcal{Y}, \widehat{\Theta}^{l-1}\right), \tag{10}$$

In case of a hybrid system, the lower bound Equation (9) is represented using the law of iterated expectations:

$$\mathcal{Q}\left(\Theta, \widehat{\Theta}^{l-1}\right) = \mathbb{E}_{\mathcal{R}}\left[\mathbb{E}_{\mathcal{X}|\mathcal{R}}\left[\mathcal{L}(\Theta) \mid \mathcal{Y}, \widehat{\Theta}^{l-1}\right]\right], \tag{11}$$

where the inner expectation is taken over the continuous-valued states conditioned on the mode, and the outer expectation is taken over the modes of the Markov chain [43, 44]. Evaluating Equation (11) constitutes the expectation step (E-step) of the algorithm. MLEs of unknown parameters are then obtained by maximising the computed expectation:

$$\widehat{\Theta}^{l} = \arg\max_{\Theta} \mathcal{Q}\left(\Theta, \widehat{\Theta}^{l-1}\right). \tag{12}$$

Evaluating Equation (12) is the maximisation step (M-step) of the algorithm, since maximising the lower bound maximises the log-likelihood in Equation (8). The algorithm is initialised with the user-define initial point of $\widehat{\Theta}^{0}$ that can be obtained by solving a Least-Squares or ML problem for the system under the assumption that all sensors are in the interactive mode. Then the two steps are iterated until the convergence of either the lower bound or MLE values. Convergence of the EM under general conditions is established in Ref. [45]. For the algorithms with a stochastic approximation of the expectations such as the one used in our framework, convergence properties were investigated in Ref. [46].

3.2 | The likelihood function

Recall that under the Assumption 3, initial state $\boldsymbol{x}_0$ and the mode $\boldsymbol{r}_0$ are known for each agent. Then the joint *pdf* of the complete dataset across all sampling points for K agents is given by

$$p(\mathcal{Z} \mid \Theta) = \prod_{k=1}^{K} \prod_{t=1}^{T_k} \left[p\left(\boldsymbol{y}_t^k \mid \boldsymbol{x}_t^k\right) \Phi\left(\boldsymbol{r}_{t+1}^k \mid \boldsymbol{r}_t^k\right) p\left(\boldsymbol{x}_{t+1}^k \mid \boldsymbol{x}_t^k, \boldsymbol{r}_t^k, \boldsymbol{\theta}\right)\right]. \tag{13}$$

Since there are no interaction between agents, their data are mutually independent and the hidden data *pdf* Equation (10) can be partitioned as

$$\boldsymbol{q}(\mathcal{R}, \mathcal{X}) = \prod_{k=1}^{K} q^k\left(\mathbf{r}^k, \mathbf{x}^k\right),$$

where each factor $q^k(\cdot) = p\left(\cdot \mid \mathbf{y}^k, \widehat{\Theta}^{l-1}\right)$ denotes the joint marginalised *pdf* of the relevant hidden variables for the kth agent. Hence, the lower bound of the joint log-likelihood function for K agents is viewed as a sum of individual $\mathcal{Q}$-functions:

$$\mathcal{Q}\left(\Theta, \widehat{\Theta}^{l-1}\right) = \sum_{k=1}^{K} \mathcal{Q}^k\left(\Theta, \widehat{\Theta}^{l-1}\right). \tag{14}$$

where the term corresponding to an individual agent conforms to Equation (11) and is represented by the integral.

$$\mathcal{Q}^k\left(\Theta, \widehat{\Theta}^{l-1}\right) = \sum_{\mathbf{r}^k} \int_{\mathbf{x}^k|\mathbf{r}^k} q^k\left(\mathbf{r}^k, \mathbf{x}^k\right) \log p\left(\mathbf{r}^k, \mathbf{x}^k, \mathbf{y}^k\right) d\mathbf{x}^k, \tag{15}$$

where the sum $\sum_{\mathbf{r}^k}[\cdot]$ is over the mode sequence and the integral $\int_{\mathbf{x}^k|\mathbf{r}^k}[\cdot]$ is over the state sequence conditioned on the mode sequence.

From substituting the complete data *pdf* in Equation (14) by Equation (13) the following expression arises

$$\begin{aligned}
&\mathcal{Q}\left(\Theta, \widehat{\Theta}^{l-1}\right) \\
&= \sum_{k=1}^{K} \left\{ \sum_{\mathbf{r}^k} \int_{\mathbf{x}^k|\mathbf{r}^k} \left\{ q^k\left(\mathbf{r}^k, \mathbf{x}^k\right) \sum_{t=0}^{T^k} \log p\left(\boldsymbol{y}_t^k \mid \boldsymbol{x}_t^k\right) \right\} d\mathbf{x}^k + \right. \\
&+ \sum_{\mathbf{r}^k} \int_{\mathbf{x}^k|\mathbf{r}^k} \left\{ q^k\left(\mathbf{r}^k, \mathbf{x}^k\right) \sum_{t=0}^{T^k} \log \Phi\left(\boldsymbol{r}_{t+1}^k \mid \boldsymbol{r}_t^k\right) \right\} d\mathbf{x}^k + \\
&\left. + \sum_{\mathbf{r}^k} \int_{\mathbf{x}^k|\mathbf{r}^k} \left\{ q^k\left(\mathbf{r}^k, \mathbf{x}^k\right) \sum_{t=0}^{T^k} \log p\left(\boldsymbol{x}_{t+1}^k \mid \boldsymbol{x}_t^k, \boldsymbol{r}_t^k, \boldsymbol{\theta}\right) \right\} d\mathbf{x}^k \right\}.
\end{aligned} \tag{16}$$

Acknowledging the Markovian nature of both state and mode evolution and the causal relationships defined by Assumptions 1 and 4, we can further marginalise the hidden data *pdf* over all unused variables in Equation (16) to obtain the following

$$\begin{aligned}
\mathcal{Q}\left(\Theta, \widehat{\Theta}^{l-1}\right) = \sum_{k,t} \Bigg\{ & \int_{\boldsymbol{x}_t^k} \left\{ q^k\left(\boldsymbol{x}_t^k\right) \log p\left(\boldsymbol{y}_t^{kd} \mid \boldsymbol{x}_t^k\right) \right\} d\boldsymbol{x}_t^k + \\
& + \sum_{\boldsymbol{r}_{t+1}^k} \sum_{\boldsymbol{r}_t^k} \left\{ q^k\left(\boldsymbol{r}_{t+1}^k, \boldsymbol{r}_t^k\right) \log \Phi\left(\boldsymbol{r}_{t+1}^k \mid \boldsymbol{r}_t^k\right) \right\} + \\
& + \sum_{\boldsymbol{r}_t^k} \int_{\boldsymbol{x}_{t+1}^k|\boldsymbol{r}_t^k} \int_{\boldsymbol{x}_t^k} \left\{ q^k\left(\boldsymbol{x}_{t+1}^k, \boldsymbol{x}_t^k, \boldsymbol{r}_t^k\right) \right. \\
& \left. \log p\left(\boldsymbol{x}_{t+1}^k \mid \boldsymbol{x}_t^k, \boldsymbol{r}_t^k, \boldsymbol{\theta}\right) \right\} d\boldsymbol{x}_{t+1}^k d\boldsymbol{x}_t^k \Bigg\},
\end{aligned} \tag{17}$$

where the outer sum is over the full time sequence for all agents $\sum_{k,t}\{\cdot\} \triangleq \sum_{k=1}^{K}\sum_{t=0}^{T_k}\{\cdot\}$. The expression in Equation (17) is separable with respect to to unknown parameters

$$\mathcal{Q}\left(\Theta, \widehat{\Theta}^{l-1}\right) = \mathcal{Q}_{\Phi} + \mathcal{Q}_{\boldsymbol{\theta}} + c, \tag{18}$$

where the constant c denotes all terms independent of unknown parameters. Note that the last term in Equation (17) constitutes the expectation of a distribution of two continuous random variables with a joint probability conditioned on the mode $\boldsymbol{r}_t^k$. Then, by factorising the hidden data *pdf*s we can express the constituent terms as follows.

$$\mathcal{Q}_{\Phi} = \sum_{j,i=1}^{N}\sum_{k,t} P\left(\boldsymbol{r}_{t+1}^k = i, \boldsymbol{r}_t^k = j \mid \mathbf{y}^k, \widehat{\Theta}^{l-1}\right)\log \boldsymbol{\phi}_{ji} \tag{19a}$$

$$\mathcal{Q}_{\boldsymbol{\theta}} = \sum_{j=1}^{N}\sum_{k,t} P\left(\boldsymbol{r}_t^k = j \mid \mathbf{y}^k, \widehat{\Theta}^{l-1}\right)\mathbb{E}_{(j)}\left[\log p\left(\boldsymbol{x}_{t+1}^k \mid \boldsymbol{x}_t^k, \boldsymbol{\theta}\right)\right], \tag{19b}$$

The expression Equation (19a) follows from the definition of the discrete variable *pdf* $q^k\left(\boldsymbol{r}_{t+1}^k, \boldsymbol{r}_t^k\right)$. In Equation (19b), the conditional expectation denotes

$$\mathbb{E}_{(j)}[\cdot] \triangleq \mathbb{E}\left[\cdot \mid \boldsymbol{r}_t^k = j, \mathbf{y}^k, \widehat{\Theta}^{l-1}\right],$$

for which the corresponding hidden data *pdf* is factorisable as follows

$$q_{(j)}^k\left(\boldsymbol{x}_{t+1}^k, \boldsymbol{x}_t^k\right) = q^k\left(\boldsymbol{x}_{t+1}^k \mid \boldsymbol{x}_t^k, \boldsymbol{r}_t^k = j\right)q^k\left(\boldsymbol{x}_t^k\right). \tag{20}$$

We denote the mode association probabilities in Equaiton (19b) as

$$\mu_{t|T^k}^k(j) \triangleq P\left(\boldsymbol{r}_t^k = j \mid \mathbf{y}^k, \Theta^l\right) \geq 0,$$

$$\sum_{j=1}^{N}\mu_{t|T^k}^k(j) = 1$$

that serve as weighting coefficients for the conditional expectations.

3.3 | Maximisation step

All constituent terms of the lower bound Equation (18) are linear with respect to the unknown parameters and thus can be maximised in the closed form. Here we provide expressions for the unknown parameter MLEs in terms of sufficient statistics that will be evaluated during the expectation step.

Recall the input affine structure of continuous state dynamics Equation (7) and expand the log-likelihood in $\mathcal{Q}_{\boldsymbol{\theta}}$ as follows

$$\mathcal{Q}_{\boldsymbol{\theta}} = \sum_{j=1}^{N}\sum_{k,t}\mu_{t|T^k}^k(j)\mathbb{E}_{(j)}\left[\left(\boldsymbol{x}_{t+1}^k - f_{(j)}\left(\boldsymbol{x}_t^k\right) - \widetilde{g}_{(j)}\boldsymbol{\theta}\right)^{\top}\cdot \cdot\Sigma_{(j)}\left(\boldsymbol{x}_{t+1}^k - f_{(j)}\left(\boldsymbol{x}_t^k\right) - \widetilde{g}_{(j)}\boldsymbol{\theta}\right)\right], \tag{21}$$

where all constants are omitted and where

$$\Sigma_{(j)} \triangleq \left(\mathbf{G}_{(j)}^{\dagger}\right)^{\top}\mathbf{Q}^{-1}\mathbf{G}_{(j)}^{\dagger}.$$

Further expansion shows that only a few terms in Equation (21) are a function of $\boldsymbol{\theta}$. The parameter MLEs are obtained by taking the partial derivative of Equation (21) with respect to $\boldsymbol{\theta}$ and setting it to zero

$$\frac{\partial \mathcal{Q}_{\boldsymbol{\theta}}}{\partial \boldsymbol{\theta}} = S_{t,t+1}^{(1)} - S_t^{(2)} - S_t^{(3)}\boldsymbol{\theta} = 0, \tag{22}$$

where the introduced sufficient statistics correspond to the expectations of the constituent terms taken over marginalised smoothing *pdf*s.

$$S_{t,t+1}^{(1)} = \sum_{j=1}^{N}\sum_{k,t}\mu_{t|T^k}^k(j)\left\{\mathbb{E}_{(j)}\left[\widetilde{g}_{(j)}^{\top}\left(\boldsymbol{x}_t^k\right)\Sigma_{(j)}\boldsymbol{x}_{t+1}^k\right]\right\} \tag{23a}$$

$$S_t^{(2)} = \sum_{j=1}^{N}\sum_{k,t}\mu_{t|T^k}^k(j)\left\{\mathbb{E}\left[\widetilde{g}_{(j)}^{\top}\left(\boldsymbol{x}_t^k\right)\Sigma_{(j)}f_{(j)}\left(\boldsymbol{x}_t^k\right)\right]\right\} \tag{23b}$$

$$S_t^{(3)} = \sum_{j=1}^{N}\sum_{k,t}\mu_{t|T^k}^k(j)\left\{\mathbb{E}\left[\widetilde{g}_{(j)}^{\top}\left(\boldsymbol{x}_t^k\right)\Sigma_{(j)}\widetilde{g}_{(j)}\left(\boldsymbol{x}_t^k\right)\right]\right\} \tag{23c}$$

where the subscripts in the left-hand side correspond to those of the states over which the expectation is taken. It can be seen that only $S_{t,t+1}^{(1)}$ is a function of two subsequent states and its corresponding expectation is taken over mode conditioned *pdf* Equation (20), whereas expectations in $S_t^{(2)}$ and $S_t^{(3)}$ depend only on the current state and therefore these *pdf*s are marginalised over the current agent mode.

Assuming that the statistics in Equation (23) are computed during the expectation step at the lth iteration, we obtain a closed-form expression for the field model parameters

$$\widehat{\boldsymbol{\theta}}^l = \left(S_t^{(3)}\right)^{-1}\left(S_{t,t+1}^{(1)} - S_t^{(2)}\right). \tag{24}$$

Furthermore, the second partial derivative of the $\mathcal{Q}$-function defined by $S_t^{(3)}$ is clearly a negative definite owing to its auto-product structure, which verifies that the new parameter estimate is located at a maximum, global or local.

The closed-form solution for the transition probability matrix arises from constrained maximisation of $\mathcal{Q}_{\Phi}$.

$$\widehat{\boldsymbol{\phi}}_{ji}^l = \frac{S_{j,i}^{(4)}}{\sum_{h=1}^{N}S_{j,h}^{(4)}}, \tag{25}$$

where the sufficient statistic is the joint probability of the agent assuming any two modes j, i at two consecutive time instances

$$S^{(4)}_{\mathrm{j,i}} = \sum_{\mathrm{k,t}} \mathrm{P}\left(\boldsymbol{r}^{\mathrm{k}}_{\mathrm{t+1}} = \mathrm{i}, \boldsymbol{r}^{\mathrm{k}}_{\mathrm{t}} = \mathrm{j} \mid \mathbf{y}^{\mathrm{k}}, \Theta\right), \tag{26}$$

Noting the Markovian property of the system, we express the sufficient statistic in terms of smoothed mode probabilities as follows

$$S^{(4)}_{\mathrm{j,i}} = \mu^{\mathrm{k}}_{\mathrm{t-1|T^k}}(\mathrm{j})\mu^{\mathrm{k}}_{\mathrm{t|T^k}}(\mathrm{i} \mid \mathrm{j}), \tag{27}$$

where the first factor is defined by Equation (21), and the second factor is the smoothed conditional probability $\mu^{\mathrm{k}}_{\mathrm{t|T^k}}(\mathrm{i} \mid \mathrm{j}) \triangleq \mathrm{P}\left(\boldsymbol{r}^{\mathrm{k}}_{\mathrm{t+1}} = \mathrm{i} \mid \boldsymbol{r}^{\mathrm{k}}_{\mathrm{t}} = \mathrm{j}, \mathbf{y}^{\mathrm{k}}, \Theta\right)$. This representation requires that we preserve the full transition kernel structure at the smoothing stage during the expectation step [47].

3.4 | Expectation step

The challenge of the expectation step is two-fold: to provide a tractable solution for the MM smoothing problem and to approximate non-linear functions of the continuous-valued states Equation (23). We propose separating these approximations at two levels to circumvent the known problems of JMNLS smoothing and reduce computational costs. First we deal with a jump Markov structure using a classical IMM scheme with a bank of extended Kalman filters in forward recursion and an extended RTS smoothers in the backward recursion. Here we employ a solution proposed in Ref. [38] that explicitly computes mode probabilities required in $S^{(1)}_{\mathrm{t,t+1}}$ and $S^{(4)}_{\mathrm{j,i}}$ at the backward stage using an approximate backward transition kernel $\widetilde{\Phi} = \left\{\widetilde{\phi}_{\mathrm{ij}}\right\}$. The backward recursion is summarised in Algorithm 1.

At the second level of approximation, we consider two approaches to computing the non-linear expectations in Equation (23):

- A1: Numerically approximate hidden data *pdf* using MC sampling from smoothing distributions [41].
- A2: Use the state estimate from the IMM smoother in a MF type approximation of the expectations.

To illustrate these approaches, we assume a generic non-linear function of the hidden state $\rho\left(\boldsymbol{x}^{\mathrm{k}}_{\mathrm{t}}\right)$ with the expectation defined by the integral over the hidden state *pdf*.

$$\mathbb{E}\left[\rho\left(\boldsymbol{x}^{\mathrm{k}}_{\mathrm{t}}\right)\right] = \int_{\boldsymbol{x}^{\mathrm{k}}_{\mathrm{t}}} \rho\left(\boldsymbol{x}^{\mathrm{k}}_{\mathrm{t}}\right) q\left(\boldsymbol{x}^{\mathrm{k}}_{\mathrm{t}}\right) d\boldsymbol{x}^{\mathrm{k}}_{\mathrm{t}}. \tag{28}$$

A1: MC sampling. This approach is based on providing a point-mass approximation of the hidden data *pdf*.

$$q\left(\boldsymbol{x}^{\mathrm{k}}_{\mathrm{t}}\right) \approx \sum_{i=1}^{L} \omega^{\mathrm{k}}_{i,\mathrm{t}} \delta_{\widetilde{\boldsymbol{x}}^{\mathrm{k}}_{i,\mathrm{t}}}\left(\boldsymbol{x}^{\mathrm{k}}_{\mathrm{t}}\right),$$

where $\left\{\widetilde{\boldsymbol{x}}^{\mathrm{k}}_{i,\mathrm{t}}\right\}_{i=1}^{L}$ is the particle system sampled from some proposal density

$$\widetilde{\boldsymbol{x}}^{\mathrm{k}}_{i,\mathrm{t}} \sim \widetilde{q}\left(\boldsymbol{x}^{\mathrm{k}}_{\mathrm{t}}\right), \tag{29}$$

and the important weights $\omega^{\mathrm{k}}_{i,\mathrm{t}}$ are computed to account for discrepancy between the true and proposal density.

$$\omega^{\mathrm{k}}_{i,\mathrm{t}} \propto \frac{q\left(\boldsymbol{x}^{\mathrm{k}}_{\mathrm{t}}\right)}{\widetilde{q}\left(\boldsymbol{x}^{\mathrm{k}}_{\mathrm{t}}\right)}.$$

Algorithm 1 Iteration of the IMM RTS smoother.

Input: Mode-conditioned states and covariances, filtered $\left(\boldsymbol{x}^{\mathrm{k}}_{\mathrm{t|t,j}}, \boldsymbol{P}^{\mathrm{k}}_{\mathrm{t|t,j}}\right)$ and smoothed $\left(\boldsymbol{x}^{\mathrm{k}}_{\mathrm{t+1|T^k,i}}, \boldsymbol{P}^{\mathrm{k}}_{\mathrm{t+1|T^k,i}}\right)$; Mode probabilities, filtered $\left(\mu^{\mathrm{k}}_{\mathrm{t|t}}(\mathrm{j})\right)$ and smoothed $\left(\mu^{\mathrm{k}}_{\mathrm{t+1|T}}(\mathrm{i})\right)$, $\mathrm{j}, \mathrm{i} \in \mathbb{M}$.

1: **for** j ← 1, N **do**

2: Approximate backward transition kernel

$$\widetilde{\phi}_{\mathrm{ij}} = \frac{1}{e_{\mathrm{i}}}\phi_{\mathrm{ji}}\mu^{\mathrm{k}}_{\mathrm{t|t}}(\mathrm{j}), \quad e_{\mathrm{i}} = \sum_{\mathrm{h}}^{\mathrm{N}} \phi_{\mathrm{hj}}\mu^{\mathrm{k}}_{\mathrm{t+1|T^k}}(\mathrm{h}).$$

3: Compute smoothing conditional probabilities

$$\mu^{\mathrm{k}}_{\mathrm{t|T^k}}(\mathrm{i} \mid \mathrm{j}) = \frac{1}{d_{\mathrm{j}}}\widetilde{\phi}_{\mathrm{ij}}\mu^{\mathrm{k}}_{\mathrm{t+1|T^k}}(\mathrm{i}), \quad d_{\mathrm{j}} = \sum_{\mathrm{h}}^{\mathrm{N}} \widetilde{\phi}_{\mathrm{hj}}\mu^{\mathrm{k}}_{\mathrm{t+1|T^k}}(\mathrm{h}).$$

4: Mixing prior states to obtain $\left(\boldsymbol{x}^{\mathrm{k}}_{\mathrm{t+1|t,j}}, \boldsymbol{P}^{\mathrm{k}}_{\mathrm{t+1|t,j}}\right)$

5: Run a mode-matched RTS smoother to obtain mode-conditioned state and covariance, $\boldsymbol{x}^{\mathrm{k}}_{\mathrm{t|T^k}}(\mathrm{j}), \boldsymbol{P}^{\mathrm{k}}_{\mathrm{t|T^k}}(\mathrm{j})$; and mode likelihood $\mathcal{L}_{\mathrm{t|T^k}}(\mathrm{j})$.

6: Compute smoothing mode probabilities

$$\mu^{\mathrm{k}}_{\mathrm{t|T^k}}(\mathrm{j}) = \frac{1}{c}\mathcal{L}_{\mathrm{t|T^k}}(\mathrm{j})\mu^{\mathrm{k}}_{\mathrm{t|t}}(\mathrm{j}), \quad c = \sum_{\mathrm{j}=1}^{\mathrm{N}} \mathcal{L}_{\mathrm{t|T^k}}(\mathrm{j})\mu^{\mathrm{k}}_{\mathrm{t|t}}(\mathrm{j}).$$

7: **end for**

8: Merge states and covariances

$$\boldsymbol{x}^{\mathrm{k}}_{\mathrm{t|T^k}} = \sum_{\mathrm{j}=1}^{\mathrm{N}} \mu^{\mathrm{k}}_{\mathrm{t|T^k}}(\mathrm{j})\boldsymbol{x}^{\mathrm{k}}_{\mathrm{t|T^k}}(\mathrm{j}),$$

$$\boldsymbol{P}^{\mathrm{k}}_{\mathrm{t|T^k}} = \sum_{\mathrm{j}=1}^{\mathrm{N}} \mu^{\mathrm{k}}_{\mathrm{t|T^k}}(\mathrm{j})\left(\boldsymbol{P}^{\mathrm{k}}_{\mathrm{t|T^k}}(\mathrm{j}) + \left(\boldsymbol{x}^{\mathrm{k}}_{\mathrm{t|T^k}}(\mathrm{j}) - \boldsymbol{x}^{\mathrm{k}}_{\mathrm{t|T^k}}\right)(\cdot)^{\mathrm{T}}\right).$$

Another attractive feature of the IMM-ERTS smoother in this context is that it provides Gaussian approximations for the merged state *pdf*s that can be used as proposal densities in Equation (29): The proposal density marginalised over mode is the merged smoothing *pdf*.

$$\widetilde{q}\left(\boldsymbol{x}_{\mathrm{t}}^{\mathrm{k}}\right)=\mathcal{N}\left(\widehat{\boldsymbol{x}}_{\mathrm{t}|\mathrm{T}^{\mathrm{k}}}^{\mathrm{k}},\boldsymbol{P}_{\mathrm{t}|\mathrm{T}^{\mathrm{k}}}^{\mathrm{k}}\right) \tag{30}$$

while the true density is a Gaussian mixture with the estimated probabilities as weights.

$$q\left(\boldsymbol{x}_{\mathrm{t}}^{\mathrm{k}}\right)=\sum_{(\mathrm{j})}^{\mathrm{N}}\mu_{\mathrm{t}|\mathrm{T}^{\mathrm{k}}}^{\mathrm{k}}(\mathrm{j})\mathcal{N}\left(\widehat{\boldsymbol{x}}_{\mathrm{t}|\mathrm{T}^{\mathrm{k}}}^{\mathrm{k}}(\mathrm{j}),\boldsymbol{P}_{\mathrm{t}|\mathrm{T}^{\mathrm{k}}}^{\mathrm{k}}(\mathrm{j})\right). \tag{31}$$

On the other hand, mode-conditioned expectations can be approximated by MC sampling directly from the smoothing *pdf* corresponding to each mode.

$$q_{(\mathrm{j})}\left(\boldsymbol{x}_{\mathrm{t}}^{\mathrm{k}}\right)=\mathcal{N}\left(\widehat{\boldsymbol{x}}_{\mathrm{t}|\mathrm{T}^{\mathrm{k}}}^{\mathrm{k}}(\mathrm{j}),\boldsymbol{P}_{\mathrm{t}|\mathrm{T}^{\mathrm{k}}}^{\mathrm{k}}(\mathrm{j})\right),\quad \mathrm{j}\in\mathbb{M}. \tag{32}$$

Since the proposal densities are already smoothed, we can sample directly from the corresponding density at each time instead of propagating the particle system in backward recursion that would be required by a particle smoother.

Particle systems sampled from densities Equations (30) and (32) are used to approximate the expectation Equation (28) as follows. Expectations marginalised over mode are computed using the IS:

$$\mathbb{E}\left[\rho\left(\boldsymbol{x}_{\mathrm{t}}^{\mathrm{k}}\right)\right]\approx\frac{1}{L}\sum_{i=1}^{L}\omega_{i,\mathrm{t}}^{\mathrm{k}}\rho\left(\overset{\sim}{\boldsymbol{x}}_{i,\mathrm{t}+1}^{\mathrm{k}}\right). \tag{33}$$

In case of mode-conditioned expectation such as $S_{\mathrm{t},\mathrm{t}-1}^{(1)}$ in Equation (23), the expectation is approximated by sampling from all factors of Equation (20) and averaging.

$$\mathbb{E}_{(\mathrm{j})}\left[\rho\left(\boldsymbol{x}_{\mathrm{t}+1}^{\mathrm{k}},\boldsymbol{x}_{\mathrm{t}}^{\mathrm{k}}\right)\right]\approx\frac{1}{L^2}\sum_{i=1}^{L}\sum_{b=1}^{L}\omega_{i,\mathrm{t}}^{\mathrm{k}}\rho\left(\overset{\sim}{\boldsymbol{x}}_{b,\mathrm{t},\mathrm{j}}^{\mathrm{k}},\overset{\sim}{\boldsymbol{x}}_{i,\mathrm{t}}^{\mathrm{k}}\right), \tag{34}$$

where

$$\left\{\overset{\sim}{\boldsymbol{x}}_{b,\mathrm{t}+1,\mathrm{j}}^{\mathrm{k}}\right\}_{b=1}^{L}\sim q_{(\mathrm{j})}\left(\boldsymbol{x}_{\mathrm{t}+1}^{\mathrm{k}}\right)$$

$$\left\{\omega_{i,\mathrm{t}}^{\mathrm{k}}\overset{\sim}{\boldsymbol{x}}_{i,\mathrm{t}}^{\mathrm{k}}\right\}_{i=1}^{L}\sim\widetilde{q}\left(\boldsymbol{x}_{\mathrm{t}}^{\mathrm{k}}\right)$$

A2: MF. If the environment is approximated by low-bandwidth basis functions that have wide support, then $\rho\left(\boldsymbol{x}_{\mathrm{t}}^{\mathrm{k}}\right)$ is a low-bandwidth in comparison to the *pdf* of the estimated agent position at any given time. The expectation integral is dominated by the mean $\widehat{\boldsymbol{x}}_{\mathrm{t}}^{\mathrm{k}}=\mathbb{E}\left[\boldsymbol{x}_{\mathrm{t}}^{\mathrm{k}}\right]$ that satisfies $\partial q\left(\boldsymbol{x}_{\mathrm{t}}^{\mathrm{k}}\mid\mathrm{y}^{\mathrm{k}},\widehat{\Theta}^{\mathrm{i}}\right)/\partial\boldsymbol{x}|_{\overset{\sim}{\boldsymbol{x}}_{\mathrm{t}}^{\mathrm{k}}}=0$, since the other factor is nearly constant in the vicinity of $\widehat{\boldsymbol{x}}_{\mathrm{t}}^{\mathrm{k}}$. This results in a MF type approximation of an expectation integral by its value at the mean point [48]:

$$\mathbb{E}\left[\rho\left(\boldsymbol{x}_{\mathrm{t}}^{\mathrm{k}}\right)\right]\approx\rho\left(\mathbb{E}\left[\boldsymbol{x}_{\mathrm{t}}^{\mathrm{k}}\right]\right), \tag{35}$$

$$\mathbb{E}_{(\mathrm{j})}\left[\rho\left(\boldsymbol{x}_{\mathrm{t}+1}^{\mathrm{k}},\boldsymbol{x}_{\mathrm{t}}^{\mathrm{k}}\right)\right]\approx\rho\left(\mathbb{E}_{(\mathrm{j})}\left[\boldsymbol{x}_{\mathrm{t}}^{\mathrm{k}}\right],\mathbb{E}\left[\boldsymbol{x}_{\mathrm{t}+1}^{\mathrm{k}}\right]\right). \tag{36}$$

While this is a more crude approximation than the simulation-based one, it allows the evaluation of expressions in Equation (23) without additional computations.

3.5 | Implementation details

The resulting algorithm is initialised with computing the gradient of the basis function grid for each measured agent position $\widehat{\boldsymbol{\varphi}}_{\mathrm{t}+1}^{\mathrm{k}}=\boldsymbol{\varphi}\left(\boldsymbol{y}_{\mathrm{t}+1}^{\mathrm{k}}\right)$ and setting $\widehat{\boldsymbol{\theta}}^{0}=0$, while the initial estimate of $\widehat{\Phi}^{0}$ is set to $0.5\mathbb{I}_2$. The estimation procedure is summarised in Algorithm 2. As an ML estimator, the developed algorithm arrives at a point estimate of unknown parameters in a finite number of iterations but does not guarantee that the estimate corresponds to the global maximum of the log-likelihood.

The IMM state estimation requires running N filters in forward time and N smoothers in backward time. The computational complexity of employed filters and smoothers will depend on the way model non-linearities are addressed. The asymptotic costs of the MF-type and MC approximation of summary statistics in the E-step are $O(NKTMd^2)$ and $O(LNKTMd^2)$, respectively, with L denoting the number of particles. The computational cost of field estimation in the M-step is dominated by $O(M^3)$, where M is the number of B-splines.

4 | SIMULATION STUDY

4.1 | Data generation

The performance of the proposed algorithm is assessed through MC simulation of several migration patterns generated in the 2-D gradient field. Each scenario is simulated 100 times with different realisations of the process noise and with the same parameters of the global field. The environment is modelled using a 4 × 4 grid of bivariate tensor product cubic B-splines $\beta(s_1, s_2)$ cardinally spaced on the map of size 1000 × 1000 arbitrary units (a.u.). Each MC experiment simulates the migration patterns of K = 100 passive agents whose trajectories are observed for T^{k} = 100 time instances or until the agent leaves the field of influence. The interaction is described by a system with linear structure.

Algorithm 2 Approximate estimation framework.

Input: Observation set, $\mathcal{Y}$; hypothesised models, $\mathbb{M}$; initial model probabilities, Π; convergence threshold, ϵ.
Output: Smoothed agent states, $\mathcal{X}$; smoothed mode probabilities, μ; estimated model parameters, $\widehat{\Theta}$.

```
Initialise parameter vector Θ̂^0;
while (l ≤ l_max) and ¬(convergence) do
  for k ← 1, K do
    IMM-EKF in forward time
    for t ← 1, T do
      IMM-ERTS backward recursion (Algorithm 1)
      A1: Obtain proposal densities (32)-(31)
      Sampling from estimated pdfs:
        MC : {x̃^k_{i,t,j}}_{b=1}^L ~ q_(j)(x^k_t),   j = 1, ..., M.
        IS : {ω_i, x̃^k_{i,t}}_{i=1}^L ~ q̃(x^k_t).
      Approximate expectations using Equations (33) and (34);
      A2: Approximate Equation (23) using Equations (35) and (36);
    end for
  end for
  Estimate Θ̂^l using Equations (24) and (25);
  Check convergence of the parameter vector Θ̂;
end while
```

$$\boldsymbol{r}_{\mathrm{t}}^{\mathrm{k}} \sim \Phi\left(\boldsymbol{r}_{\mathrm{t}}^{\mathrm{k}} \mid \boldsymbol{r}_{\mathrm{t}}^{\mathrm{k}}\right) \tag{37a}$$

$$\boldsymbol{x}_{\mathrm{t}+1}^{\mathrm{k}} = \mathbf{A}_{(\boldsymbol{r}_{\mathrm{t}}^{\mathrm{k}})}\left(\boldsymbol{x}_{\mathrm{t}}^{\mathrm{k}}\right) + \mathbf{B}_{(\boldsymbol{r}_{\mathrm{t}}^{\mathrm{k}})}\boldsymbol{u}_{\mathrm{t}}^{\mathrm{k}} + \mathbf{G}_{(\boldsymbol{r}_{\mathrm{t}}^{\mathrm{k}})}\boldsymbol{w}_{\mathrm{t}}^{\mathrm{k}} \tag{37b}$$

$$\boldsymbol{y}_{\mathrm{t}}^{\mathrm{k}} = \mathbf{C}\boldsymbol{x}_{\mathrm{t}}^{\mathrm{k}} + \boldsymbol{v}_{\mathrm{t}}^{\mathrm{k}}, \tag{37c}$$

where $\boldsymbol{u}_{\mathrm{t}}^{\mathrm{k}}$ is defined by Equation (5). Note that because the state of an agent enters the basis function decomposition of the field, the model Equation (37b) remains non-linear with respect to the state.

Each agent can assume one of two modes: the responsive mode in which the object responds to the acting environment.

$$\mathbf{A}_{(1)} = \begin{bmatrix} \mathbb{I}_2 & T\mathbb{I}_2 \\ \mathbb{O}_2 & \mathbb{I}_2 - T\rho_{(1)}\mathbb{I}_2 \end{bmatrix} \mathbf{B}_{(1)} = \begin{bmatrix} \frac{T^2}{2}\mathbb{I}_2 \\ T\mathbb{I}_2 \end{bmatrix} \mathbf{G}_{(1)} = \begin{bmatrix} \frac{T^2}{2}\mathbb{I}_2 \\ T\mathbb{I}_2 \end{bmatrix}, \tag{38}$$

and the non-responsive mode in which an agent is not influenced by the environment.

$$\mathbf{A}_{(2)} = \begin{bmatrix} \mathbb{I}_2 & T\mathbb{I}_2 \\ \mathbb{O}_2 & \mathbb{I}_2 - T\rho_{(2)}\mathbb{I}_2 \end{bmatrix} \mathbf{B}_{(2)} = \begin{bmatrix} \mathbb{O}_2 \\ \mathbb{O}_2 \end{bmatrix} \mathbf{G}_{(2)} = \begin{bmatrix} \frac{T^2}{2}\mathbb{I}_2 \\ T\mathbb{I}_2 \end{bmatrix}, \tag{39}$$

where $T = 1$ min is the time increment and $\mathbb{I}_2$ is the identity matrix and $\mathbb{O}_2$ is a zero matrix of size 2×2. The presented model is the Euler–Maruyama discretisation of the biased random walk with resistance to the environment that is commonly used to describe particle and cell motion. In the transition matrix $\mathbf{A}$, the term $\mathbb{I}_2 - T\rho\mathbb{I}_2$ corresponds to the reversion to mean in the O-U process describing the velocity of a large Brownian particle, while the matrix $\mathbf{B}$ in the first mode introduces bias in response to the environment.

The rate of the reversion to mean has been set to $\rho_{(1)} = 0.3$ for the sensing mode and $\rho_{(2)} = 0.7$ for the desensitised mode. The process noise covariances are set to $\mathbf{Q}_{(1)} = 0.2\mathbb{I}_2$ a.u.^{2}/min^4 and $\mathbf{Q}_{(2)} = 0.5\mathbb{I}_2$ a.u.^{2}/min^4, The measurement noise covariance is set to $\mathbf{R} = \mathbb{I}_2$ a.u.^{2}. Initial velocity estimates are arbitrarily assumed to be zero with uncertainty covariance $\boldsymbol{P}_0 = \mathbb{I}_2$ a.u.^{2}/min^4. Initial mode probabilities for the IMM filter are set to $\boldsymbol{\pi} = [0.5, 0.5]$ to ensure no knowledge of the initially correct model. The mode transition probability matrix Φ is set to

$$\begin{bmatrix} \phi_{11} & \phi_{12} \\ \phi_{21} & \phi_{22} \end{bmatrix} = \begin{bmatrix} 0.9 & 0.1 \\ 0.2 & 0.8 \end{bmatrix}. \tag{40}$$

The described system is used to generate the agent of migration patterns with uniformly distributed starting point. The examples of generated tracking data for each scenario are demonstrated in Figure 2. The generated trajectories are then processed with two versions of the estimation framework: the first version utilised MF approximation of non-linear sufficient statistics, while the second version relied on the importance sampling with $L = 100$ particles generated from each proposal distribution.

4.2 | Estimation results

The estimation results for the field model are presented in Figure 3a,c. The mean and standard deviation of parameter MLEs are obtained from 50 MC simulations. Recalling Remark 2 about inferring the gradient and not the field itself, we use absolute bias between the true field and the one constructed with mean estimates to assess the performance of the estimation framework. As shown in Figure 3b,d, Both algorithms are able to reconstruct the gradient that is consistent with the modelled one, however the MF-based EM understates the slope of the field. The highest bias is observed in the area with the highest field magnitude. This can be explained by the fact that the true gradient in that area is rather small and its influence on the agents is comparable with the magnitude of process noise. This results in assignment of high probabilities to the diffusing mode for many agents in that area, reducing

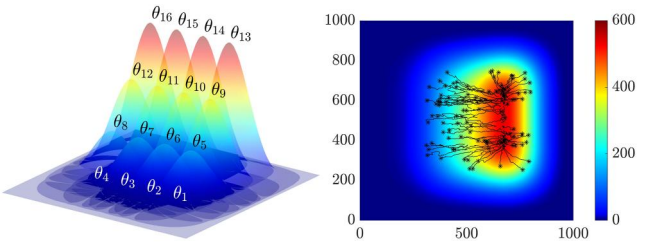

(a) B-spline grid. (b) Agent trajectories.

FIGURE 2 Generative model and the example agent trajectories. (a) The grid of basis functions with corresponding scaling coefficients used to model the potential field: $\Theta_{1:4} = 10$, $\Theta_{5:8} = 100$, $\Theta_{9:12} = 190$, $\Theta_{13:16} = 290$. (b) All agents enter the field at random positions (*).

the information about the local gradient. The result might indicate that the localisation of the sensing agents and their spread in the region of interest is one of the key contributing factors to the accuracy of environment inference. Further investigation of varying movement patterns may be required. The IS-based method overstates field magnitude, but the bias of the estimate is nearly constant in the region of interest and thus can be explained by Remark 2.

Table 1 summarises selected statistics obtained with both MF-based and IS-based algorithms. The last column of the table includes the present computing time required to one EM iteration of each method.[1] It can be seen from the table that MF-based EM achieves the accuracy similar to the IS-based EM at nearly of the computational cost that is proportional to the number of particles used in sampling. The comparable results of two methods can be explained by low measurement noise variance: agent position estimates obtained from the IMM smoother will not change significantly with iterations of the EM algorithm. We can conclude that since in most practical applications the noise-to-signal ratio in tracking of agent positions is small, the MF-based algorithm can be used without significant loss of accuracy.

The inference of the mode switching process from the tracking data is performed both in the M-step, where the transition probability matrix is estimated, and in the E-step, where the most probable mode sequence can be obtained from estimated mode probabilities. The example results presented in Figure 4 demonstrate that the estimates converge to the true values. The mean and 3σ deviation interval for the transition probabilities are calculated from the sample of 50 MC simulations (see Figure 4c). Successful estimation of mode transition probabilities is the result of having a model structure where behavioural modes are distinguishable from one another. It can be seen in Figure 4e, however, that some short-term changes of the mode are not detected by the framework. Under the scenarios in which the change in the true mode is reversed within a short time interval, the smoothed mode probabilities do not change significantly to reflect this change

[1]All computations are performed using MATLAB Parallel Computing Toolbox on UoS HPC cluster. Full specifications can be found at https://docs.hpc.shef.ac.uk/en/latest/sharc/cluster_specs.html.

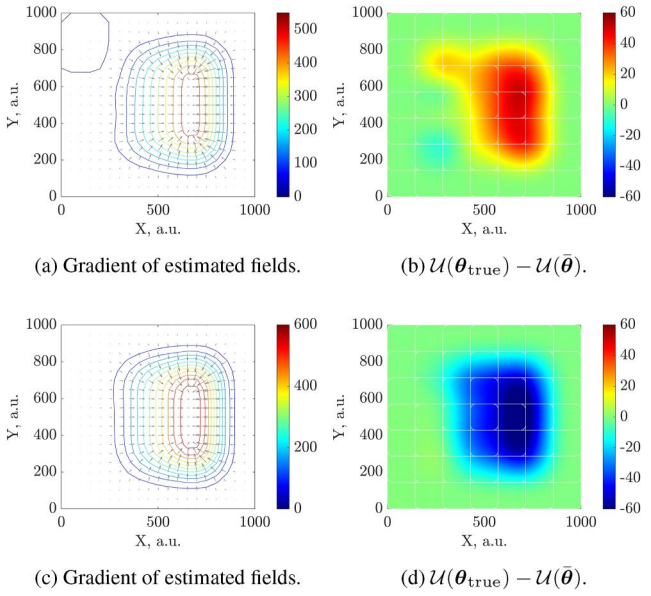

(a) Gradient of estimated fields. (b) $\mathcal{U}(\boldsymbol{\theta}_{\text{true}}) - \mathcal{U}(\bar{\boldsymbol{\theta}})$.

(c) Gradient of estimated fields. (d) $\mathcal{U}(\boldsymbol{\theta}_{\text{true}}) - \mathcal{U}(\bar{\boldsymbol{\theta}})$.

FIGURE 3 Environment inference. Left: the potential field constructed with mean maximum likelihood estimate of B-spline coefficients averaged over 50 MC realisations $\bar{\boldsymbol{\theta}}_m = \sum_{i_{MC}=1}^{50} \hat{\boldsymbol{\theta}}^{i_{MC}}$, where i_{MC} is the simulation index. Right: absolute bias. Colourbars normalised to one scale. (a, b) Results obtained using MF-based EM. (c, d) Results obtained using IS-based EM. EM, expectation-maximisation; MF, mean-field.

(see times $t = 30$, 60, and 70 min in Figure 4d). Thus is the result of a fundamental trade-off between detecting abrupt changes in the mode and smoothing noisy processes in the smoothing procedure.

5 | APPLICATION STUDY: CELL MIGRATION

5.1 | Neutrophil chemotaxis

The applicability of the developed framework is demonstrated on the dataset from Ref. [11] where the migration of white blood cells (neutrophils) during the inflammatory reaction in zebrafish larvae is analysed. The inflammation is triggered by the injury of the fish tail fin. In the initial stages of the inflammatory event, neutrophils migrate to the injury site in response to the chemical attractant (ChA) that is generated at the cut area and spreads out into the tissue. The cells known to travel up the ChA gradient and arrive to the inflammation site within the first several hours post injury [49]. In the experiment, neutrophils are tracked via video microscopy with time increment of 30 s. For the purpose of testing the framework, these cells are considered to be the sensing agents, and their trajectories shown in Figure 5a constitute the observation dataset $\mathcal{Y}$. Cell velocities are not measured, but they constitute hidden data $\mathcal{X}$. The environment of interest, $\mathcal{U}$, is the concentration of the ChA.

It has been established experimentally that neutrophils transition between different behavioural modes while migrating through the tissue [14]. Several works suggest varying number of modes, with the unifying idea that at certain periods the cells

TABLE 1 Selected MLE statistics

	Max std		Min std		Max bias		Min bias		
Methods	**Value**	**Coeff.**	**Value**	**Coeff.**	**Value**	**Coeff.**	**Value**	**Coeff.**	**Time, s**
MF	34.427	θ_1	7.192	θ_{10}	32.831	θ_{15}	1.484	θ_6	737.35
IS	29.052	θ_4	11.689	θ_{11}	39.106	θ_{15}	1.019	θ_3	1276.6

Abbreviations: MF, mean-field; MLE, maximum likelihood estimate.

stop interacting with the environment due to receptor oversaturation. In this example, we assume that each cell can assume one of the three modes: responsive mode (M1) that characterises interaction with the environment, diffusing mode (M2) for active cells with receptor oversaturation, and stationary mode (M3) that characterises behaviour of cells either waiting to be dispatched to the tissue or those arrived to the wound. These modes are coresspond to the states of the Markov chain $\mathbb{M} = \{1, 2, 3\}$. We utilise the SSM structure Equation (37) introduced in the previous section. The responsive mode is described by the model with the structure Equation (38), which corresponds to a model of single cell motion described in Ref. [49]. The other two modes are modelled by O-U process Equation (39) with different noise amplitudes.

The hidden chemoattractant field in this case has been approximated by a 5×4 grid of B-splines. The time increment between observations is $t = 2$ min with the observation noise covariance set to $2\mathbb{I}_2\ \mu m^2$. Mode-specific coefficients of reversion to mean are set to $\rho_{(1)} = 0.3$, $\rho_{(2)} = 0.5$, $\rho_{(3)} = 0.5$, and process noise covariances are set to $\mathbf{Q}_{(1)} = 2\mathbb{I}_2\ \mu m^2/\text{min}^4$, $\mathbf{Q}_{(2)} = 2\mathbb{I}_2\ \mu m^2/\text{min}^4$, $\mathbf{Q}_{(3)} = 0.5\mathbb{I}_2\ \mu m^2/\text{min}^4$, with an initial field parameter estimate $\Theta = 0$, and the initial mode transition probability is defined as follows: $\phi_{ji} = 0.8$, $j = i$, $\phi_{ij} = 0.1$, $j \neq i \quad \forall j, i \in \mathbb{M}$. The data is processed using the EM algorithm with MF-type approximation.

5.2 | Chemoattractant inference

The results of applying the estimation framework to the cell tracking data for an individual zebrafish larvae are presented in Figure 5. While it is impossible to determine whether the magnitude of the field has been estimated correctly, the estimated gradient is consistent with the experiments that measure the concentration of attractants near the wound of the tail fin [4]. Besides, a sparse polynomial basis provides a consistent gradient—in the areas without cell tracks the estimated concentration of the ChA is uniformly low.

The framework appears to make a clear distinction between different migratory modes. For example, it can be seen in Figure 5d that the probabilities of an agent being in the responsive mode are normally close to one or zero. The MLEs of mode transition probabilities illustrated in Figure 5b indicate that the diffuse mode may be an intermediate state between the responsive and stationary modes, as the MLE ϕ_{22} is small compared to other diagonal elements of the transition matrix. Since only cells in the first mode contain information about the environment, the increase in estimated concentration is observed starting from the middle of the tail fin, where more neutrophils start aligning with the direction of the wound as shown in Figure 5c.

The following behavioural pattern can be established from the estimates of mode probabilities. Multiple cells start in the fish's lower body at a stationary mode waiting to be released into

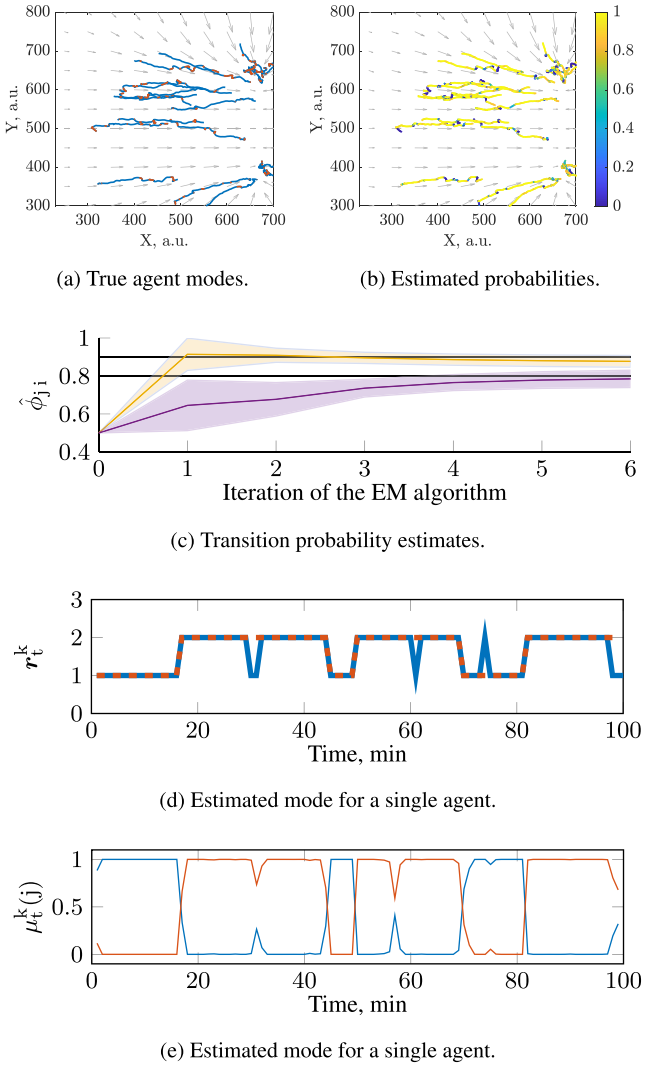

(a) True agent modes. (b) Estimated probabilities.

(c) Transition probability estimates.

(d) Estimated mode for a single agent.

(e) Estimated mode for a single agent.

FIGURE 4 Agent behaviour inference. (a) True agent positions and modes of agents against the true gradient: $j = 1$ (——) and $j = 2$ (——). (b) Estimated agent positions colour coded according to the probability of being in a responsive mode. (c) Transition probability maximum likelihood estimates and $\pm 3\sigma$ confidence regions: $\widehat{\phi}_{11}$ (——) and $\widehat{\phi}_{22}$ (——). (d) The estimated mode sequence for an individual agent: estimated mode (▪ ▪ ▪) against the mode of the generative model (▬). (e) Smoothed mode probabilities for $j = 1$ (——) and $j = 2$ (——).

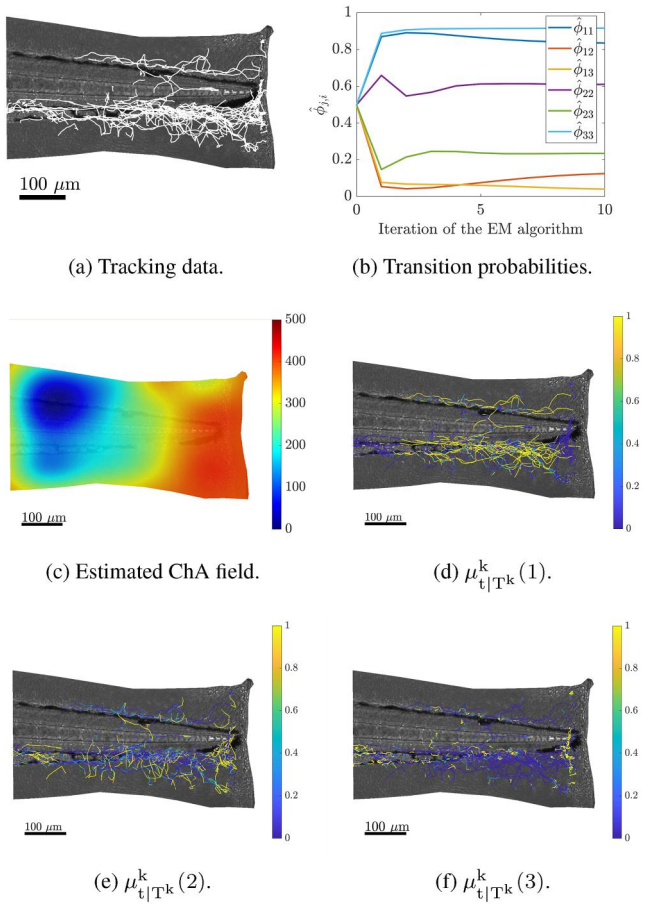

FIGURE 5 Estimation results for the neutrophil migration patterns. (a) Experimental data used for field estimation. (c) Estimated transition probabilities between three modes. (b) The estimated concentration field of the chemical attractant in the zebrafish tailfin. (d) Responsive mode probabilities for each track. (e) Diffusing mode probabilities for each track. (f) Stationary mode probabilities for each track.

the tissue. Once activated, neutrophils first diffuse away from the starting point in search of the gradient. Upon sensing an uneven concentration, they switch to the responsive mode and rapidly migrate up the gradient (see Figure 5d). Occasional changes back to the diffusive mode are seen in Figure 5e; they may be the result of sporadic receptor desensitisation to the chemoattractant or obstacles within the tissue. Upon entering the wound site, the area starting at an ~100 μm away from the wound, the neutrophils switch back to the diffusive mode and eventually slow down to a stationary mode (see Figure 5f). These results illustrates how the developed estimation framework can provide an insight into both the underlying environment affecting cell population and the changing behaviour of the individual cells.

6 | CONCLUSION

This paper introduces a modelling and estimation framework that deals with a novel problem, in which the global environment driving multiple passive agents is estimated from their observed movement. The dynamics of an individual agent moving in response to its environment is described by an input affine JMNLS. The switching nature of the model reflects heterogeneous behaviour of agents observed in many applications, while the affine input term incorporates the local influence of the global environment on the agent. The basis function decomposition of the environment renders the linear-in-parameters global model that can be estimated from localised trajectory data.

The proposed hybrid system is embedded into the maximum likelihood estimation framework to estimate the functional form of the unknown environment and the transition probability matrix associated with agent behavioural modes. Since the estimation is performed in the presence of hidden data, an EM solution is derived. The expectation step combines IMM smoothing and with two approaches to approximating the sufficient statistics, importance sampling and MF approximation. These approximations of the necessary statistics are then used in the maximisation step to compute the estimates of unknown parameters in closed form.

The simulation examples reveal that the MF type approximation of the sufficient statistics in the EM algorithm achieves accuracy comparable with the simulation-based approximations at a smaller computational cost. The framework identifies the mode sequence of agents which indicates that IMM is sufficient for JMNLS estimation in cases where dynamical model of each mode is known. The framework is then used to analyse the migration of white blood cells in the inflammatory response in a living animal. The estimate of the attractant concentration field driving cell migration conforms with the concentration patterns demonstrated in experimental literature. The case study illustrates the applicability of the novel formulation that captures the changing behaviour of sensing agents in unknown environments.

AUTHOR CONTRIBUTIONS

Conceptualization: Anastasia Kadochnikova and Visakan Kadirkamanathan. Data curation: Anastasia Kadochnikova. Formal analysis: Anastasia Kadochnikova. Funding acquisition: Anastasia Kadochnikova and Visakan Kadirkamanathan. Investigation: Anastasia Kadochnikova and Visakan Kadirkamanathan. Methodology: Anastasia Kadochnikova and Visakan Kadirkamanathan. Project administration: Anastasia Kadochnikova. Resources: Visakan Kadirkamanathan. Software: Anastasia Kadochnikova. Supervision: Visakan Kadirkamanathan. Validation: Anastasia Kadochnikova. Visualization: Anastasia Kadochnikova. Writing – original draft: Anastasia Kadochnikova. Writing – review & editing: Anastasia Kadochnikova and Visakan Kadirkamanathan.

ACKNOWLEDGEMENT

This research was funded by the Full Departmental Scholarship of ACSE Department, University of Sheffield.

CONFLICT OF INTEREST

Authors declare no conflict of interest.

DATA AVAILABILITY STATEMENT

The developed MATLAB script and the experimental data used in the application study are available from the corresponding author upon reasonable request.

ORCID

Anastasia Kadochnikova https://orcid.org/0000-0002-5416-7848

REFERENCES

1. Fabbiano, R., de Wit, C.C., Garin, F.: Source localization by gradient estimation based on Poisson integral. Automatica 50(6), 1715–1724 (2014). https://doi.org/10.1016/j.automatica.2014.04.029
2. Matveev, A.S., et al.: Robot navigation for monitoring unsteady environmental boundaries without field gradient estimation. Automatica 62, 227–235 (2015). https://doi.org/10.1016/j.automatica.2015.09.003
3. Frishman, A., Ronceray, P.: Learning force fields from stochastic trajectories. Phys. Rev. X 10(2), 021009 (2020). https://doi.org/10.1103/physrevx.10.021009
4. Kadirkamanathan, V., et al.: The neutrophil's eye-view: inference and visualisation of the chemoattractant field driving cell chemotaxis in vivo. PLoS One 7(4), e35182 (2012). https://doi.org/10.1371/journal.pone.0035182
5. Jones, P.J.M., et al.: Inference of random walk models to describe leukocyte migration. Phys. Biol. 12(6), 1–12 (2015). https://doi.org/10.1088/1478-3975/12/6/066001
6. Patle, B.K., et al.: A review: on path planning strategies for navigation of mobile robot. Defence Technol. 15(4), 582–606 (2019). https://doi.org/10.1016/j.dt.2019.04.011
7. Murphy, J., Godsill, S.: Simultaneous localization and mapping for non-parametric potential field environments. In: 2012 Workshop on Sensor Data Fusion: Trends, Solutions, Applications (SDF), pp. 1–6 (2012)
8. Gan, L., et al.: Ship path planning based on safety potential field in inland rivers. Ocean Eng. 260, 111928 (2022). https://doi.org/10.1016/j.oceaneng.2022.111928
9. Liepe, J., et al.: Calibrating spatio-temporal models of leukocyte dynamics against *in vivo* live-imaging data using approximate Bayesian computation. Integr. Biol. 4(3), 335–345 (2012). https://doi.org/10.1039/c2ib00175f
10. Rossi, L.A., Krishnamachari, B., Kuo, C.C.J.: Distributed parameter estimation for monitoring diffusion phenomena using physical models. In: 2004 First Annual IEEE Communications Society Conference on Sensor and Ad Hoc Communications and Networks, 2004, pp. 460–469. IEEE SECON 2004 (2004)
11. Kadochnikova, A., et al.: Estimation of hidden chemoattractant field from observed cell migration patterns. IFAC-PapersOnLine 55(15), 766–771 (2018). https://doi.org/10.1016/j.ifacol.2018.09.161
12. Manolopoulou, I., et al.: Bayesian spatio-dynamic modeling in cell motility studies: learning nonlinear taxic fields guiding the immune response. J. Am. Stat. Assoc. 107(499), 855–865 (2012). https://doi.org/10.1080/01621459.2012.655995
13. Rapoport, I., Oshman, Y.: Efficient fault tolerant estimation using the IMM methodology. IEEE Trans. Aero. Electron. Syst. 43(2), 492–508 (2007). https://doi.org/10.1109/taes.2007.4285349
14. Boyarsky, A., Noble, P.: A Markov chain characterization of human neutrophil locomotion under neutral and chemotactic conditions. Can. J. Physiol. Pharmacol. 55(1), 1–6 (1977). https://doi.org/10.1139/y77-001
15. Armond, J.W., et al.: A stochastic model dissects cell states in biological transition processes. Sci. Rep. 4(1), 3692 (2014). https://doi.org/10.1038/srep03692
16. Costa, O.L.V., Fragoso, M.D., Marques, R.P.: Discrete-time Markov jump linear systems. In: Probability and its Applications. Springer London (2006)
17. Dempster, A.P., Laird, N.M., Rubin, D.B.: Maximum likelihood from incomplete data via the EM algorithm. J. Roy. Stat. Soc. B 39(1), 1–38 (1977). https://doi.org/10.1111/j.2517-6161.1977.tb01600.x
18. Tugnait, J.K.: Adaptive estimation and identification for discrete systems with Markov jump parameters. IEEE Trans. Automat. Control 27(5), 1054–1065 (1982). https://doi.org/10.1109/tac.1982.1103061
19. Logothetis, A., Krishnamurthy, V., Holst, J.: A Bayesian EM algorithm for optimal tracking of a manoeuvring target in clutter. Signal Process. 82(3), 473–490 (2002). https://doi.org/10.1016/s0165-1684(01)00198-0
20. Dewar, M., Kadirkamanathan, V.: A canonical space-time state space model: state and parameter estimation. IEEE Trans. Signal Process. 55(10), 4862–4870 (2007). https://doi.org/10.1109/tsp.2007.896245
21. Bar-Shalom, Y., Li, X.R.: Estimation and Tracking: Principles, Techniques, and Software. Artech House (1993)
22. Rong Li, X., Jilkov, V.P.: Survey of maneuvering target tracking. Part V. multiple-model methods. IEEE Trans. Aero. Electron. Syst. 41(4), 1255–1321 (2005). https://doi.org/10.1109/taes.2005.1561886
23. Doucet, A., Gordon, N.J., Krishnamurthy, V.: Particle filters for state estimation of jump Markov linear systems. IEEE Trans. Signal Process. 49(3), 613–624 (2001). https://doi.org/10.1109/78.905890
24. Rahmathullah, A.S., Svensson, L., Svensson, D.: Two-filter Gaussian mixture smoothing with posterior pruning. In: 17th International Conference on Information Fusion (FUSION), pp. 1–8. IEEE, Salamanca (2014)
25. Blom, H.A.P., Bar-Shalom, Y.: The interacting multiple model algorithm for systems with Markovian switching coefficients. IEEE Trans. Automat. Control 33(8), 780–783 (1988). https://doi.org/10.1109/9.1299
26. Johnston, L.A., Krishnamurthy, V.: An improvement to the interacting multiple model (IMM) algorithm. IEEE Trans. Signal Process. 49(12), 2909–2923 (2001). https://doi.org/10.1109/78.969500
27. Chen, R., Liu, J.S.: Mixture Kalman filters. J. Roy. Stat. Soc. B Stat. Methodol. 62(3), 493–508 (2000). https://doi.org/10.1111/1467-9868.00246
28. Svensson, A., Schön, T.B., Lindsten, F.: Identification of jump Markov linear models using particle filters. In: 53rd IEEE Conference on Decision and Control, pp. 6504–6509. IEEE, Los Angeles (2014)
29. Logothetis, A., Krishnamurthy, V.: Expectation maximization algorithms for MAP estimation of jump Markov linear systems. IEEE Trans. Signal Process. 47(8), 2139–2156 (1999). https://doi.org/10.1109/78.774753
30. Chen, B., et al.: Mobile location estimator in a rough wireless environment using extended Kalman-based IMM and data fusion. IEEE Trans. Veh. Technol. 58(3), 1157–1169 (2009). https://doi.org/10.1109/tvt.2008.928649
31. Qian, H., An, D., Xia, Q.: IMM-UKF based land-vehicle navigation with low-cost GPS/INS. In: The 2010 IEEE International Conference on Information and Automation, pp. 2031–2035. IEEE, Harbin (2010)
32. Li, W., Jia, Y.: Location of mobile station with Maneuvers using an IMM-based cubature Kalman filter. IEEE Trans. Ind. Electron. 59(11), 4338–4348 (2012). https://doi.org/10.1109/tie.2011.2180270
33. Saha, S., Hendeby, G.: Rao-Blackwellized particle filter for Markov modulated nonlinear dynamic systems. In: IEEE Workshop on Statistical Signal Processing Proceedings, pp. 272–275. IEEE, Gold Coast (2014)
34. Driessen, H., Boers, Y.: An efficient particle filter for jump Markov nonlinear systems. In: IET Conference Proceedings, pp. 19–22. IET, Brighton (2004)
35. Lopez, R., Danès, P.: A fixed-interval smoother with reduced complexity for jump Markov nonlinear systems. In: 17th International Conference on Information Fusion (FUSION), pp. 1–8 (2014)
36. Lopez, R., Danès, P.: Low-complexity IMM smoothing for jump Markov nonlinear systems. IEEE Trans. Aero. Electron. Syst. 53(3), 1261–1272 (2017). https://doi.org/10.1109/taes.2017.2669698
37. Koch, W.: Fixed-interval retrodiction approach to Bayesian IMM-MHT for maneuvering multiple targets. IEEE Trans. Aero. Electron. Syst. 36(1), 2–14 (2000). https://doi.org/10.1109/7.826308
38. Nadarajah, N., et al.: IMM forward filtering and backward smoothing for Maneuvering target tracking. IEEE Trans. Aero. Electron. Syst. 48(3), 2673–2678 (2012). https://doi.org/10.1109/taes.2012.6237617
39. Liu, Y., et al.: On the fixed-interval smoothing for jump Markov nonlinear systems. In: 2022 25th International Conference on Information Fusion (FUSION), pp. 1–8. IEEE, Linköping (2022)

40. Ozkan, E., et al.: Recursive maximum likelihood identification of jump Markov nonlinear systems. IEEE Trans. Signal Process. 63(3), 754–765 (2015). https://doi.org/10.1109/tsp.2014.2385039
41. Lindsten, F., Schön, T.B.: Backward simulation methods for Monte Carlo statistical inference. Found. Trends Mach. Learn. 6(1), 1–143 (2013). https://doi.org/10.1561/2200000045
42. Meng, X.L., Rubin, D.B.: Maximum likelihood estimation via the ECM algorithm. Biometrika 20(2), 267–278 (1993). https://doi.org/10.1093/biomet/80.2.267
43. Blackmore, L., et al.: Model learning for switching linear systems with autonomous mode transitions. In: 2007 46th IEEE Conference on Decision and Control, pp. 4648–4655. IEEE, New Orleans (2007)
44. Yildirim, S., Singh, S.S., Doucet, A.: An online expectation–maximization algorithm for changepoint models. J. Comput. Graph. Stat. 22(4), 906–926 (2013). https://doi.org/10.1080/10618600.2012.674653
45. Wu, J.C.F.: On the convergence properties of the EM algorithm. Ann. Stat. 11(1), 95–103 (1983). https://doi.org/10.1214/aos/1176346060
46. Delyon, B., Lavielle, M., Moulines, E.: Convergence of a stochastic approximation version of the EM algorithm. Ann. Stat. 27(1), 94–128 (1999). https://doi.org/10.1214/aos/1018031103
47. Orguner, U., Demirekler, M.: Maximum likelihood estimation of transition probabilities of jump Markov linear systems. IEEE Trans. Signal Process. 56(10), 5093–5108 (2008). https://doi.org/10.1109/tsp.2008.928936
48. Kastella, K.: Event-averaged maximum likelihood estimation and mean-field theory in multitarget tracking. IEEE Trans. Automat. Control 40(6), 1070–1074 (1995). https://doi.org/10.1109/9.388686
49. Stokes, C.L., Lauffenburger, D.A., Williams, S.K.: Migration of individual microvessel endothelial cells: stochastic model and parameter measurement. J. Cell Sci. 99(2), 419–430 (1991). https://doi.org/10.1242/jcs.99.2.419

How to cite this article: Kadochnikova, A., Kadirkamanathan, V.: Estimation of potential field environments from heterogeneous behaviour of sensing agents. IET Signal Process. e12181 (2023). https://doi.org/10.1049/sil2.12181